Available online at www.sciencedirect.com
SCIENCE DIRECT®
Carbohydrate Research 340 (2005) 1826–1840
Carbohydrate RESEARCH

Structural analysis of xyloglucans in the primary cell walls of plants in the subclass *Asteridae*

Matt Hoffman, Zhonghua Jia, Maria J. Peña, Michael Cash, April Harper, Alan R. Blackburn, II, Alan Darvill and William S. York*

Complex Carbohydrate Research Center and Department of Biochemistry and Molecular Biology, University of Georgia, 315 Riverbend Road, Athens, GA 30602-4712, USA

Received 9 March 2005; accepted 29 April 2005
Available online 21 June 2005

Abstract—The structures of xyloglucans from several plants in the subclass Asteridae were examined to determine how their structures vary in different taxonomic orders. Xyloglucans, solubilized from plant cell walls by a sequential (enzymatic and chemical) extraction procedure, were isolated, and their structures were characterized by NMR spectroscopy and mass spectrometry. All campanulids examined, including *Lactuca sativa* (lettuce, order Asterales), *Tenacetum ptarmiciflorum* (dusty miller, order Asterales), and *Daucus carota* (carrot, order Apiales), produce typical xyloglucans that have an XXXG-type branching pattern and contain α-D-Xyl*p*-, β-D-Gal*p*-(1→2)-α-D-Xyl*p*-, and α-L-Fuc*p*-(1→2)-β-D-Gal*p*-(1→2)-α-D-Xyl*p*- side chains. However, the lamiids produce atypical xyloglucans. For example, previous analyses showed that *Capsicum annum* (pepper) and *Lycopersicon esculentum* (tomato), two species in the order Solanales, and *Olea europaea* (olive, order Lamiales) produce xyloglucans that contain arabinosyl and galactosyl residues, but lack fucosyl residues. The XXGG-type xyloglucans produced by Solanaceous species are less branched than the XXXG-type xyloglucan produced by *Olea europaea*. This study shows that *Ipomoea pupurea* (morning glory, order Solanales), *Ocimum basilicum* (basil, order Lamiales), and *Plantago major* (plantain, order Lamiales) all produce xyloglucans that lack fucosyl residues and have an unusual XXGGG-type branching pattern in which the basic repeating core contains five glucose subunits in the backbone. Furthermore, *Neruim oleander* (order Gentianales) produces an XXXG-type xyloglucan that contains arabinosyl, galactosyl, and fucosyl residues. The appearance of this intermediate xyloglucan structure in oleander has implications regarding the evolutionary development of xyloglucan structure and its role in primary plant cell walls.

Keywords: Xyloglucan; Asteridae; Polysaccharide; NMR spectroscopy; Structural characterization; O-Acetylation; Taxonomy

1. Introduction

The primary wall that surrounds cells in growing and succulent plant tissues plays a critical role in balancing the osmotic forces in living cells, preventing them from bursting but still allowing them to grow in a controlled, oriented manner.[1,2] Thus, by controlling the morphological development of individual plant cells, cell walls directly regulate plant growth and morphology. The primary cell wall consists of cellulose microfibrils embedded in a matrix composed primarily of polysaccharides.[1] The major components of this matrix are pectins and hemicelluloses. The most abundant hemicellulosic polysaccharide in the primary cell wall of most vascular plants is xyloglucan (XyG), which is synthesized in the Golgi and exported to the apoplasm in soluble form.[3] XyG spontaneously and avidly binds to the surface of cellulose microfibrils, and is thereby incorporated into the xyloglucan/cellulose network, which forms a major load bearing structure in the primary cell walls of most higher plants.[2,4]

XyGs have a cellulosic backbone composed of (1→4)-linked β-D-Glc*p* residues to which α-D-Xyl*p* residues are linked at O-6. XyGs are highly branched polysaccharides, that have been classified as 'XXXG-type' or

* Corresponding author. Tel.: +1 706 542 4628; fax: +1 706 542 4412; e-mail: will@ccrc.uga.edu

0008-6215/$ - see front matter © 2005 Elsevier Ltd. All rights reserved.
doi:10.1016/j.carres.2005.04.016

'XXGG-type',[5] depending on the number and distribution of side chains that are attached to the backbone. XyGs containing XXXXG-type subunits, which have five β-D-Glc*p* residues in the backbone, have also been isolated from seeds.[6] The majority of higher plants produce XXXG-type XyGs, in which three of every four β-D-Glc*p* residues in the backbone have an α-D-Xyl*p* residue at O-6, and the remaining, unbranched β-D-Glc*p* residues are regularly spaced along the backbone. Typically, XXXG-type XyGs have three different side chain structures, α-D-Xyl*p*- (represented by the letter X), β-D-Gal*p*-(1→2)-α-D-Xyl*p*- (represented by the letter L), and α-L-Fuc*p*-(1→2)-β-D-Gal*p*-(1→2)-α-D-Xyl*p*- (represented by the letter F). Thus, a typical XXXG-type XyG is composed predominantly of the oligosaccharide subunits XXXG, XXFG, XXLG, and XLFG. (See Fry et al.[7] and footnotes of Table 2 for further description of this nomenclature.) As shown in Tables 1 and 2, the fucosylated XXXG-type structure is conserved in taxonomically diverse plant species, including, for example, pines (gymnosperms), legumes (dicotyledonous angiosperms), and onions (monocotyledonous angiosperms). Conservation of the α-L-Fuc*p*-(1→2)-β-D-Gal*p*-(1→2)-α-D-Xyl*p*- side chains in such a wide range of plant species suggests functional importance. However, genetically modified *A. thaliana* plants that lack the AtFut1 activity that is responsible for the transfer of α-L-Fuc*p* residues to xyloglucans appear to grow normally under greenhouse conditions.[8]

Certain Solanaceous asterids such as tobacco and tomato (see Table 1 for taxonomic classification) produce atypical XyGs that contain α-L-Ara*f* and/or β-D-Gal*p* residues but lack α-L-Fuc*p* residues (Table 2). Solanaceous XyGs also have an atypical XXGG-type branching pattern, in which two unbranched Glc residues follow two branched residues.[9,10] One of the two adjacent unbranched Glc residues often has an *O*-acetyl substituent at O-6. It is not known how the structural modifications affect the biophysical properties of the XyG, or how the plant compensates for the loss of a conserved structural feature such as fucosyl residue-containing side chains or an XXXG-type branching pattern. In order to shed light on the evolutionary processes that could have given rise to the observed structural diversity, xyloglucans from several plants in the subclass Asteridae were isolated and structurally characterized.

2. Results and discussion

Alcohol-insoluble residue (AIR), which consists primarily of cell-wall material, was prepared from the leaf tissues of several Asterid species, and two separate XyG oligosaccharide fractions were prepared from each of these AIR samples. One fraction was prepared by treating depectinated cell wall material (AIR) with a xyloglucan-specific endoglucanase (XEG), which releases XyG oligosaccharides (XyGOs) from the enzyme-accessible XyG domain in the cell wall.[11] The other fraction was prepared by extracting the XEG-treated AIR with 4 N KOH, neutralizing the extract, and treating polymeric XyG in this extract with XEG to generate oligosaccharides. The two oligosaccharide fractions were characterized by MALDI-TOF mass spectrometry and ^{1}H NMR spectroscopy. Oleander XyGOs were also reduced to the alditol form for further purification and characterization. Specific structural features of the oligosaccharides in each fraction were initially identified by their correlation to diagnostic resonances[9,12,13] in their ^{1}H NMR spectra. (See the XyG NMR database at http://www.ccrc.uga.edu/web/specdb/specdbframe.html.) New structural features, such as unusual branching patterns, were established by first-principles analysis of 2D NMR experiments, including gCOSY, NOESY, TOCSY, HSQC, and HMBC.

2.1. XyGs produced by campanulid species

^{1}H NMR spectroscopy (Fig. 1) combined with MALDI-TOF mass spectrometry (Table 3) of XyGO fractions indicates that several plant species in the campanulids (carrot, lettuce, dusty-miller) all produce typical fucosylated xyloglucans. The MALDI-TOF mass spectra of the XEG and KOH oligosaccharide fractions obtained from every campanulid examined indicate that these species produce very similar XXXG-type XyGs composed predominantly of the oligosaccharide subunits XXXG, XXLG, XXFG, and XLFG, and that these XyGs have very few *O*-acetyl substituents (Table 3). The ^{1}H NMR spectra of these fractions confirmed this conclusion (Fig. 1). For example, the presence of the α-L-Fuc*p*-(1→2)-β-D-Gal*p*-(1→2)-α-D-Xyl*p*- side chain in these XyGs is indicated by diagonostic resonances[9,12,13] at δ 5.28 (H-1 of α-L-Fuc*p*), δ 5.14 (H-1 of 2-linked α-D-Xyl*p*), and δ 4.62 (H-1 of 2-linked β-D-Gal*p*). Other resonances indicated the presence of α-D-Xyl*p*- and β-D-Gal*p*-(1→2)-α-D-Xyl*p*- side chains in these oligosaccharide fractions (Fig. 1). The ratio of the total anomeric signal integral for α-Xyl*p* residues to that of total reducing (α- and β-) Glc*p* residues was between 2.95 and 3.25, consistent with the presence of three branch points per oligosaccharide for each of the campanulid XyG fractions. These results, in combination with the mass spectral results shown in Table 3, indicate that the XyGs that were isolated from campanulid cell walls all have a typical fucosylated structure with an XXXG-type branching pattern.

2.2. XyGs produced by lamiid species

The XyG isolated from the lamiids showed much more structural diversity than those isolated from the

campanulids. Although XyGs produced by suspension-cultured cells of Solanaceous plants had been previously characterized,[9,13,14] XyGs in the leaves of two of these (tomato and sweet pepper) were characterized for comparison to leaf XyGs from other asterids. The XyG in tomato leaves is similar to that produced by cultured tomato cells,[13] but with a considerably simpler structure. The MALDI-TOF mass spectrum of the tomato leaf XEG fraction (Table 3) indicates the presence of mono-*O*-acetylated XXGG, XSGG, LSGG, LSGG, and LLGG. One-dimensional (Fig. 2) and two-dimensional (gCOSY, data not shown) spectra of this fraction included signals diagnostic for monoglycosyl (α-D-Xyl*p*-), diglycosyl (α-L-Ara*f*-(1→2)-α-D-Xyl*p*-, and β-D-Gal*p*-(1→2)-α-D-Xyl*p*-) side chains, although there was no indication of the unusual β-L-Ara*f*-(1→3)-α-L-Ara*f*-(1→2)-α-D-Xyl*p*- side chain that is found in suspension-cultured tomato cells.[9,13] *O*-Acetyl substituents were found predominantly at O-6 of the backbone β-D-Glc*p* residues, as indicated by diagnostic resonances[10] at δ 4.61 and 4.31. No resonances diagnostic for *O*-acetyl substituents on the side chains were observed, in contrast to the XyGOs from suspension-cultured tomato cells.[10] Integration of total reducing α- and β-Glc*p* H-1 signals (1.0 proton), total α-Xyl*p* H-1 signals (2.2 protons), and 6-*O*-acetyl-β-Glc*p* H-6 signals (1.1 protons) was consistent with an XXGG-type branching pattern, as has previously been shown for tomato XyG from suspension-cultured cells.[10] Signal integration also indicated that approximately 70% of the tomato leaf XyGOs contain an Ara*f*-(1→2)-α-D-Xyl*p*- side chain and 20% contain a β-D-Gal*p*-(1→2)-α-D-Xyl*p*- side chain. NMR and mass spectral results indicated that sweet pepper leaf XyG has a very similar structure, except that 78% of the pepper XyGOs contain an Ara*f*-(1→2)-α-D-Xyl*p*- side chain and 45% contain a β-D-Gal*p*-(1→2)-α-D-Xyl*p*- side chain. Partial characterization of the XyG from tobacco (*Nicotiana tabacum*) leaves indicated a structure similar to that of tomato leaf XyG except that the tobacco XyG contained very few β-D-Gal*p*-(1→2)-α-D-Xyl*p*- side chains.

Table 1. Taxonomic relationships of various plant species

Kingdom	Subkingdom	Superdivision	Division	Class	Subclass	Order	Family	Genus	Species	Table 2 Index
Plantae										
	Trachebionta (vascular plants)									
		Spermatophyta (seed plants)								
			Coniferophyta (conifers)							
				Pinopsida						
					Pinales					
						Taxodiaceae (redwood family)				
							Cryptomeria			
								japonica	japanese cedar	1
			Magnoliophyta (flowering plants)							
				Liliopsida (monocotyledons)						
					Commelinidae					
						Cyperales				
							Poaceae (grass family)			
								Hordeum	barley	2
								Oryza	sativa (rice)	3
								Zea	mays (corn)	4
					Liliidae					
						Liliales				
							Lileaceae (lily family)			
								Allium	cepa (garden onion)	5
									sativum (cultivated garlic)	6
				Magnoliopsida (dicotyledons)						
					Dilleniidae					
						Primulales				
							Primulaceae (primrose family)			
								Cyclomen	cyclomen	7
						Malvales				
							Malvaceae (mallow family)			
								Gossypium	cotton	8
						Salicales				
							Salicaceae (willow family)			
								Populus	alba (white poplar)	9
						Capparales				
							Brassicaceae			
								Arabidopsis	thaliana	23
					Rosidae					
						Rosales				
							Rosaceae (rose family)			
								Malus P. Mill	apple	10
						Euphorbiales				
							Simmondsiaceae (jojoba family)			
								Simmondsia	chinenses (jojoba)	11
						Fabales				
							Fabaceae (pea family)			
								Copaifera	langsdorfii (langsdorf copaifera)	12
								Hymenaea (hymenaea)	courbaril (stinkingtoe)	13
								Glycine Willd. (soybean)	max (soybean)	14
								Tamarindus (tamarind)	indica (tamarind)	15
								Vigna Savi (cowpea)	radiata (mung bean)	16
						Sapindales				
							Aceraceae			
								Acer	pseudoplatanus (sugar maple)	33
									more Magnoliopsida (continued in next column)	

Table 1 (*continued*)

	Magnoliopsida (dicotyledons, *continued from previous column*)									
	Asteridae									
		Ericales								
			Sapotaceae							
				Argania						
					spinosa (argan tree)					21
Campanulids		Asterales								
			Asteraceae (aster family)							
				Arctium (burrdock)						
					lappa (greater burrdock)					17
				Lactuca						
					sativa (lettuce)					18
				Tanacetum						
					ptarmiciflorum (dusty-miller)					19
		Apiales								
			Apiaceae							
				Daucus						
					carota (carrot)					20
		Gentianales								
			Apocynaceae							
				Nerium						
					oleander					22
		Lamiales								
			Lamiaceae							
				Mentha						
					piperita (peppermint)					23
				Ocimum						
					basilicum (basil)					24
			Oleaceae (olive family)							
				Olea (olive)						
					europaea (olive)					25
			Veronicaceae							
				Plantago						
					major (plantain)					26
Lamiids		Solanales								
			Convolvulaceae							
				Ipomoea						
					purpurea (morning glory)					27
			Solanaceae (potato family)							
				Capsicum						
					annuum (sweet pepper)					28
				Nicotiana (tobacco)						
					plumbaginifolia (tex-mex tobacco)					29
					tabacum (cultivated tobacco)					30
				Solanum (nightshade)						
					tuberosum (Irish potato)					31
				Lycopersicon						
					esculentum (tomato)					32

Table 2. Structures of xyloglucans in various plant species

Index	Organism	Tissue	Subunits described	Reference
1	*Cryptomeria japonica* (Japanese cedar)	Differentiating xylem	XXXG XXLG XXFG XLLG XLFG	21
2	*Hordeum* (barley)	Immature plants	XXGGG	22
3	*Oryza* (rice)	Seedling	XXGGG XGGG	18
	Rice	Suspension-cultured cells	XLXG XXXG XXG GG	23
	Rice	Hull	XG XX XXG	24
4	*Zea mays* (corn)	Shoot	XG XXG XLG	25
5	*Allium cepa* (onion)	Bulb	XLFG XXFG XXLG XXXG	26
6	*Allium sativum* (garlic)	Bulb	XLFG XXFG XXLG XXXG	26
	Hybrid (garlic/onion)	Bulb	XLFG XXFG XXLG XXXG	26
7	Cyclamen (cyclomen)	Seed	XXLG XXXG XLLG	27
8	*Gossypium* (cotton)	Cotton fiber	XLFG XXFG XXLG XXXG	28
9	*Populus alba* (poplar)	Cultured cells	XLFG XXFG XXLG XXXG	29
10	*Malus* P. Mill (apple)	Fruit	XXXG XXFG XLFG	30
	Malus P. Mill (apple)	Apple pomace	XXXG, XXFG, XLFG	31
11	*Simmondsia chinenses* (jojoba)	Seed	XXXG XXLG XLJG XXJG XLFG XXFG	32
12	*Copaifera langsdorfii*	Seed	XXXG XLXG XXLG XLLG	33
13	*Hymenaea courbaril* (stinkingtoe)	Cotyledons	(XXXG XLXG XXLG XLLG) XXXXG 50%	6
14	*Glycine max* (soybean)	Cultured cells	XXFG XXXG	34
	Glycine max (soybean)	Soybean meal	XXG XXXG XXFG XLXG XLFG	35
15	*Tamarindus indica* (tamarind)	Seed	XXXG XXLG XLLG	36
16	*Phaseolus aureus* (mung bean)	Hypocotyls	XXFG XXXG	37
	Mung bean	Hypocotyls	XLFG	38
17	*Arctium lappa* (greater burrdock aka gobo)		XLFG XXFG XXXG	39
18	*Lactuca sativa* (lettuce)	Leaves	XXXG XXFG XLFG	This paper
19	*Tanacetum ptarmiciflorum* (dusty-miller)	Leaves	XXXG XXFG XLFG	This paper
20	*Daucus carota* (carrot)	Leaves	XXXG XXFG XLFG	This paper
21	*Argania spinosa* (argan tree)	Leaves	XXXG XXFG XLXG/XXLG XLFG XUFG	40
22	*Nerium oleander*	Leaves	XLFG XXFG XXXG XLSG XXSG	This paper
23	*Arabidopsis thaliana*	Cultured cells and whole plant tissues	XLFG XXFG XXXG	41
24	*Ocimum basilicum* (basil)	Leaves	XLGGG	This paper
25	*Olea europaea* (olive)	Purple olive fruit	XXSG XLSG	15
26	*Plantago major* (plantain)	Leaves	XLGGG	This paper
27	*Ipomea Purpurea* (morning glory)	Leaves	XSGGG	This paper
28	*Capsicum* (pepper)	Leaves	XXGG XSGG	This paper
29	*Nicotiana plumbaginifolia* (tex-mex tobacco)	Cultured cells	XXGG SXGG XSGG SSGG SSGGG SXGGG XSGGG XLXG XXLG	14
30	*Nicotiana tabacum* (cultivated tobacco)	Leaves	XXGG XSGG	This paper
31	*Solanum tuberosum* (Irish potato)	Tuber	Contains arabinose	42
32	*Lycopersicon esculentum* (tomato)	Cultured cells	GXSG XXGG GSXG XSGG LXGG XTGG LSGG LLGG LTGG	13
33	*Acer pseudoplantanus* (sycamore)	Cultured cells	XLFG XXFG XXXG	12,43

XyG oligosaccharide structures are indicated using the nomenclature proposed by Fry et al.,[7] in which the structure of each backbone Glc residue and its pendant side chains are represented by a single, uppercase letter. G represents an unbranched β-D-Glc*p* residue. X represents a β-D-Glc*p* residue with a terminal α-D-Xyl*p* residue at O-6. L represents a β-D-Glc*p* residue with a β-D-Gal*p*(1→2)-α-D-Xyl*p* side chain at O-6. F represents a β-D-Glc*p* residue with an α-L-Fuc*p*(1→2)-β-D-Gal*p*(1→2)-α-D-Xyl*p* side chain at O-6. S represents a β-D-Glc*p* residue with an α-L-Ara*f*(1→2)-α-D-Xyl*p* side chain at O-6. In this paper, underlined, uppercase letters indicate the presence of an *O*-acetyl substituent on the substructure.

The widest range of side-chain structures from any species examined was found in the XyG extracted from *Nerium oleander* leaves. Resonances diagnostic for monoglycosyl (α-D-Xyl*p*-), diglycosyl (α-L-Ara*f*-(1→2)-α-D-Xyl*p*- and β-D-Gal*p*-(1→2)-α-D-Xyl*p*-) and triglycosyl (α-L-Fuc*p*-(1→2)-β-D-Gal*p*-(1→2)-α-D-Xyl*p*-) side chains are present in the 1D (Fig. 2) and 2D (gCOSY, data not shown) ^{1}H NMR spectra of the oleander XyGO fractions. This is the first example, to our knowledge, of a single XyG that contains all of these

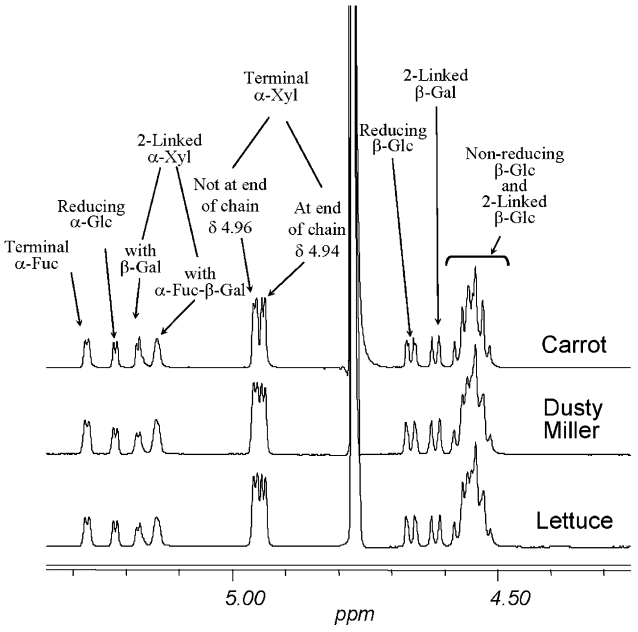

Figure 1. ^{1}H NMR spectra of XEG-extracted XyGOs from campanulid species.

side-chain structures. In order to identify specific XyGOs from oleander, the KOH fraction was reduced to generate oligoglycosyl alditols, which were separated by HPLC. Comparison of the ^{1}H NMR spectra of the purified oleander oligoglycosyl alditols to authentic standards[12,15] resulted in the identification of XXXGol, XXFGol, XLFGol, XXSGol, and XLSGol in these fractions, although XXSGol and XLSGol were not fully separated under the conditions used.

The native XyGOs in the oleander XEG fraction were also partially separated by HPLC, and several were identified by MALDI-TOF mass spectrometry (data not shown) and NMR spectroscopy. These XyGOs included XLFG, XXFG, and XXSG with an *O*-acetyl group at O-5 of the Ara residue, and XLSG also with an *O*-acetyl group at O-5 of the Ara residue, and XXFG with an *O*-acetyl group at O-6 of the Gal residue in the trisaccharide side chain. The locations of *O*-acetyl substituents in the oligosaccharides were readily determined in each case by correlating the attachment site to the precise chemical shifts of proton resonances that are deshielded by O-acetylation.[10] No resonances indicating the presence of an *O*-acetyl substituent at O-6 of the backbone β-D-Glc*p* residues were observed in these spectra. This is consistent with the exclusive detection of XXXG-type oligosaccharides in the oleander XyG, as O-acetylation of β-D-Glc*p* residues in the backbone has been observed *only* when at least two adjacent β-D-Glc*p* residues are unbranched (i.e., as in XXGG-type XyGs). The assignment of an XXXG-type structure to oleander XyG is also consistent with signal integrals obtained from the ^{1}H NMR spectra of the oleander XGOs (Table 4).

Examination of the ^{1}H NMR spectra of the tomato and oleander XyGOs suggested that analysis of the relative intensity of the resonances at δ 4.94 and δ 4.96 in these spectra would provide a convenient way to determine the branching pattern of the parent polysaccharide. The anomeric proton resonance of a terminal α-D-Xyl*p* residue that is glycosidically linked to O-6 of the β-D-Glc*p* residue at the nonreducing end of a XyGO backbone is consistently observed at δ 4.940. (See the vertical dotted line in Fig. 2.) The H-1 resonances of terminal α-D-Xyl*p* residues at other locations in the XyGO are observed at δ 4.96. Furthermore, XEG can only cleave unbranched β-D-Glc*p* residues in the XyG backbone, and in XXXG-type XyGs, this unbranched residue is almost always glycosidically linked to a β-D-Glc*p* residue that bears a terminal α-D-Xyl*p* residue at O-6. Thus, nearly all of the XyGOs produced by XEG-treatment of an XXXG-type XyG have a terminal α-D-Xyl*p* residue that gives rise to a resonance at δ 4.940. The locations of XEG-susceptible sites in XXXG-type XyGs do not depend on the presence or absence of *O*-acetyl substituents, so the relative intensity of the δ 4.94 and 4.96 resonances are not affected by pretreatment with KOH, which removes *O*-acetyl substituents from the polysaccharide. For example, approximately 55% of the terminal α-Ara*f* residues in the oleander-leaf XEG fraction are O-acetylated at O-5 (Fig. 2, Table 4), as indicated by the observation of two distinct H-1 resonances (δ 5.185 and δ 5.168) for terminal α-Ara*f* residues and two H-1 resonances (δ 5.090 and δ 5.060) for 2-linked α-Xyl*p* residues that bear the α-Ara*f* residues at O-2. When oleander XyG is extracted with KOH (Fig. 2), the signal intensity of the δ 5.168 and δ 5.090 resonances increases, and the δ 5.185 and δ 5.060 resonances are not observed, which is consistent with O-deacetylation of the α-Ara*f* residues. Nevertheless, the ^{1}H NMR spectra of the oleander XEG and KOH fractions exhibit nearly the same intensity ratio for the δ 4.94 and δ 4.96 signals (Fig. 2), indicating that, as expected for an XXXG-type XyG, O-deacetylation does not affect the XEG susceptibility of any backbone β-D-Glc*p* residues.

The intensity pattern (described above) for the δ 4.94 and δ 4.96 signals in the ^{1}H NMR spectra of XXXG-type oleander oligosaccharides is distinct from that observed for XXGG-type oligosaccharides obtained from other species, such as tomato (Fig. 2). In XXGG-type XyGs, two adjacent, unbranched β-D-Glc*p* residues are present in the backbone. In the native polysaccharide, one of these unbranched glucose residues is susceptible to XEG-catalyzed hydrolysis, but the other is usually acetylated at O-6, making it XEG-resistant. As a result, XEG-treatment of an XXGG-type XyG with endogenous *O*-acetyl substituents on the backbone generates a collection of XyGOs, the great majority of which have a terminal α-D-Xyl*p* residue at O-6 of the β-D-Glc*p* residue at the end of

Table 3. MALDI-TOFMS of leaf XyG oligosaccharide fractions

XEG fraction			KOH fraction		
m/z	Ion	Structure	*m/z*	Ion	Structure
Campanulid species					
Carrot (*Daucus carota*)					
1086	$M+Na^+$	XXXG	1087	$M+Na^+$	XXXG
			1103	$M+K^+$	XXXG
1249	$M+Na^+$	XXLG	1250	$M+Na^+$	XXLG
		XLXG			XLXG
1395	$M+Na^+$	XXFG	1396	$M+Na^+$	XXFG
			1412	$M+K^+$	XXFG
1558	$M+Na^+$	XLFG	1558	$M+Na^+$	XLFG
			1574	$M+K^+$	XLFG
Dusty miller (*Tanacetum ptarmiciflorum*)					
1086	$M+Na^+$	XXXG	1086	$M+Na^+$	XXXG
1102	$M+K^+$	XXXG	1102	$M+K^+$	XXXG
1249	$M+Na^+$	XXLG	1249	$M+Na^+$	XXLG
		XLXG			XLXG
1264	$M+K^+$	XXLG	1265	$M+K^+$	XXLG
		XLXG			XLXG
1395	$M+Na^+$	XXFG	1394	$M+Na^+$	XXFG
1410	$M+K^+$	XXFG	1411	$M+K^+$	XXFG
1437^{weak}	$M+Na^+$	XXFG-Ac			
1557	$M+Na^+$	XLFG	1557	$M+Na^+$	XLFG
1573	$M+K^+$	XLFG	1573	$M+K^+$	XLFG
1599^{weak}	$M+Na^+$	XLFG-Ac			
Lettuce (*Lactuca sativa*)					
1086	$M+Na^+$	XXXG	1087	$M+Na^+$	XXXG
1102	$M+K^+$	XXXG	1103	$M+K^+$	XXXG
1248	$M+Na^+$	XXLG	1249	$M+Na^+$	XXLG
		XLXG			XLXG
1264	$M+K^+$	XXLG	1265	$M+K^+$	XXLG
		XLXG			XLXG
1394	$M+Na^+$	XXFG	1395	$M+Na^+$	XXFG
1411	$M+K^+$	XXFG	1411	$M+K^+$	XXFG
1557	$M+Na^+$	XLFG	1558	$M+Na^+$	XLFG
1573	$M+K^+$	XLFG	1574	$M+K^+$	XLFG
Lamiid species					
Tomato (*Lycopersicon esculentum*)					
925	$M+Na^+$	XSG			
998	$M+Na^+$	XXGG-Ac			
1014	$M+K^+$	XXGG-Ac			
1130	$M+Na^+$	XSGG-Ac			
1145	$M+K^+$	XSGG-Ac			
1159	$M+Na^+$	LXGG-Ac			
1175	$M+K^+$	LXGG-Ac			
1292	$M+Na^+$	LSGG-Ac			
1308	$M+K^+$	LSGG-Ac			
1320	$M+Na^+$	LLGG-Ac			
Sweet pepper (*Capsicum annuum*)					
			926	$M+Na^+$	XSG
			942	$M+K^+$	XSG
996	$M+Na^+$	XXGG-Ac	957	$M+Na^+$	XXGG
					GXXG
1012	$M+K^+$	XXGG-Ac	973	$M+K^+$	XXGG
					GXXG
1127	$M+Na^+$	XSGG-Ac	1088	$M+Na^+$	XSGG
1144	$M+K^+$	XSGG-Ac	1105	$M+K^+$	XSGG
1158	$M+Na^+$	LXGG-Ac	1118	$M+Na^+$	LXGG
					GXXGG
1174	$M+K^+$	LXGG-Ac	1135	$M+K^+$	LXGG
					GXXGG

(*Continued on next page*)

Table 3. Sweet pepper (*Capsicum annuum*) (*continued*)

XEG fraction			KOH fraction		
m/z	Ion	Structure	*m/z*	Ion	Structure
1290	$M+Na^+$	LSGG-Ac	1251	$M+Na^+$	LSGG
					GXSGG
1306	$M+K^+$	LSGG-Ac	1267	$M+K^+$	LSGG
					GXSGG
1320	$M+Na^+$	LLGG-Ac	1281	$M+Na^+$	LLGG
					GLXGG
1336	$M+K^+$	LLGG-Ac	1297	$M+K^+$	LLGG
					GLXGG
			1414	$M+Na^+$	GLSGG
			1429	$M+K^+$	GLSGG
Oleander (*Oleander nerium*)					
1086	$M+Na^+$	XXXG	1086	$M+Na^+$	XXXG
1102	$M+K^+$	XXXG	1102	$M+K^+$	XXXG
1218	$M+Na^+$	XXSG	1218	$M+Na^+$	XXSG
1234	$M+K^+$	XXSG	1235	$M+K^+$	XXSG
1249	$M+Na^+$	XXLG	1248	$M+Na^+$	XXLG
		XLXG			XLXG
1261	$M+Na^+$	XXSG-Ac			
1276	$M+K^+$	XXSG-Ac			
1380	$M+Na^+$	XLSG	1381	$M+Na^+$	XLSG
1394	$M+Na^+$	XXFG	1395	$M+Na^+$	XXFG
1410	$M+K^+$	XXFG	1411	$M+K^+$	XXFG
1422	$M+Na^+$	XLSG-Ac			
1436	$M+Na^+$	XXFG-Ac			
1557	$M+Na^+$	XLFG	1557	$M+Na^+$	XLFG
1573	$M+K^+$	XLFG	1573	$M+K^+$	XLFG
Plantain (*Plantago major*)					
			956	$M+Na^+$	GXXG
					XXGG
1160	$M+Na^+$	GXXGG-Ac	1118	$M+Na^+$	GXXGG
					XLGG
		XLGG-Ac			GXLG
		XXGGG-Ac			XXGGG
1202	$M+Na^+$	XXGGG-Ac_2	1280^{major}	$M+Na^+$	GXLGG
1364^{major}	$M+Na^+$	XLGGG-Ac_2	1442	$M+Na^+$	GGXLGG
Morning glory (*Ipomoea pupurea*)					
1084	$M+Na^+$	GXSG	1086	$M+Na^+$	GXSG
1126	$M+Na^+$	XSGG-Ac	1102	$M+K^+$	GXSG
1198	$M+Na^+$	XXGGG-Ac_2	1248	$M+Na^+$	GXSGG
1245	$M+Na^+$	XSGGG	1265^{major}	$M+K^+$	GXSGG
		GXSGG			
1329^{major}	$M+Na^+$	XSGGG-Ac_2	1381	$M+Na^+$	GSSGG
1407	$M+Na^+$	GXSGGG	1398	$M+K^+$	GSSGG
1461	$M+Na^+$	SSGGG-Ac_2			

the main chain, giving rise to a resonance at δ 4.940. However, when an XXGG-type XyG is deacetylated by KOH extraction, both of the adjacent unbranched glucose residues become susceptible to XEG-catalyzed cleavage. This leads to the generation of XyGOs in which the β-D-Glc*p* residue at the end of the XyGO backbone does not necessarily bear an α-D-Xyl*p* residue at O-6. Therefore, when a cell-wall preparation containing an XXGG-type XyG is analyzed, the intensity ratio for the δ 4.94 and δ 4.96 resonances is likely to be significantly lower for the (O-deacetylated) oligosaccharides prepared from KOH-extracted material than for the (O-acetylated) oligosaccharides prepared by direct treatment of the AIR with XEG (Fig. 2). Thus, comparison of the signal intensity for the resonances at δ 4.94 and δ 4.96 in the XEG- and KOH-extracted XyGO fractions is a convenient way to determine whether or not a XyG has an XXXG-type branching pattern.

Two species in the order Lamiales (plantain, *Plantago major*, family Veronicaceae, and basil, *Ocimum basilicum*, family Lamiaceae) produced highly homologous XyGs that have an unexpected structure. Figure 3 shows the ^{1}H NMR spectra of the XEG and KOH fractions from plantain leaves, which are very similar

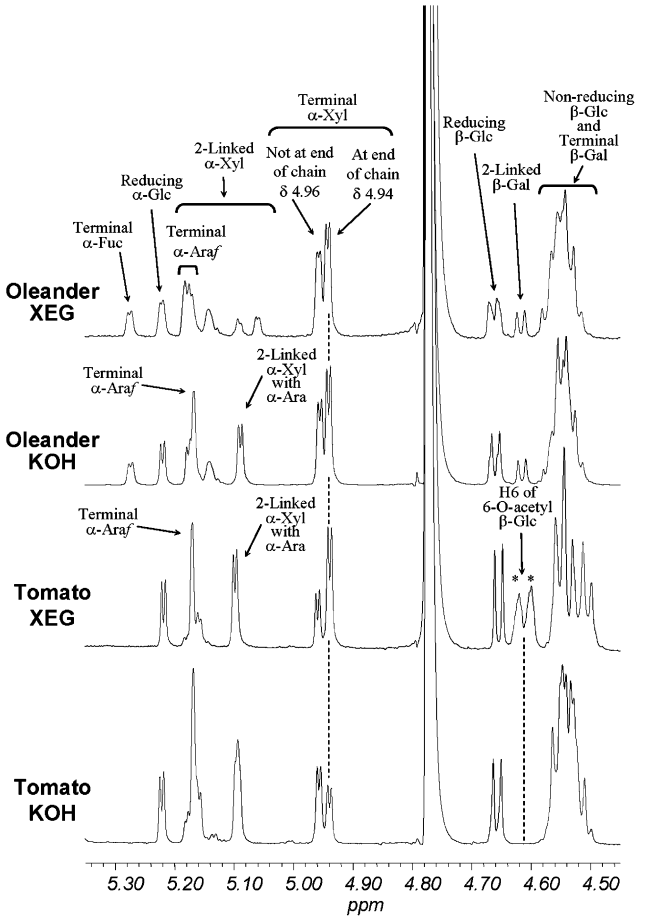

Figure 2. Effect of extraction protocol on the ratio of diagnostic resonance intensities in the ^{1}H NMR spectra of XXXG-type and XXGG-type XyGs. A resonance at δ 4.613 in the spectrum of the oligosaccharides generated by XEG-treatment of tomato cell walls indicates the presence of *O*-acetyl substituents at O-6 of β-D-Glc*p* residues in the backbone. Diagnostic crosspeak patterns in the COSY spectra readily distinguish this resonance from the resonance (δ 4.617) in the spectrum of the oleander XyG oligosaccharides due to H-1 of 2-linked β-D-Gal*p* residues.

to the spectra of the corresponding fractions obtained from basil leaves. These spectra indicate the presence of monoglycosyl (α-D-Xyl*p*-) and diglycosyl (β-D-Gal*p*-(1→2)-α-D-Xyl*p*-) side chains, but surprisingly show no indication of α-L-Fuc*p* or α-L-Ara*f* residues. A comparison of the ^{1}H NMR spectra (Fig. 3) of the XEG- and KOH-extracted XyGO fractions indicates the presence of at least two adjacent unbranched β-D-Glc*p* residues in the backbone of these XyGs. That is, the spectrum of the plantain-leaf XEG fraction contains a strong resonance at δ 4.94, indicating the presence of a terminal α-D-Xyl*p* residue at O-6 of the β-D-Glc*p* residue at the end of the main chain of most of the oligosaccharides, and a much weaker resonance at δ 4.96, indicating relatively few terminal α-D-Xyl*p* residues are attached to O-6 of internal β-D-Glc*p* residues. In contrast, the ^{1}H NMR spectrum of the plantain-leaf KOH fraction includes a strong signal at δ 4.96 and a very weak signal at δ 4.940, indicating that nearly all of the terminal α-D-Xyl*p* residues in this fraction are attached to O-6 of internal β-D-Glc*p* residues. Furthermore, integration of the H-6 resonances (e.g., δ 4.620, 4.608, 4.311, 4.293, Tables 4 and 5) diagnostic for the presence of *O*-acetyl substituents indicates that two β-D-Glc*p* residues in each oligosaccharide in the plantain-leaf XEG fraction bear an *O*-acetyl substituent at O-6. Such 6-*O*-acetyl-β-D-Glc*p* residues are resistant to hydrolysis by XEG, and yet the polysaccharide is cleaved by this enzyme, so there must be at least three unbranched β-D-Glc*p* residues in each oligosaccharide subunit of this polymer.

Due to the unusual nature of the branching pattern for the basil and plantain XyGs, the structure of the major component of the XEG-extracted XyGO fraction from plantain was determined by complete assignment of the 2D NMR spectra of this material (Table 5). gCOSY and TOCSY spectra of the fraction allowed the resonances in isolated spin systems, each corresponding to an individual glycosyl residue, to be assigned. Furthermore, long-range scalar coupling observed in the gCOSY spectra[10,13,16] provided information regarding interglycosidic linkages in the oligosaccharide (Table 6) and the attachment site of the *O*-acetyl substituents.[10] The identity of residues involved in specific glycosidic linkages was confirmed from the NOESY spectrum (Table 6), which provided information regarding the spatial proximity of anomeric protons in each glycosyl residue to protons in the aglycon, and a complete map of the interglycosidic linkage sites was obtained. The ^{13}C resonances of the oligosaccharide were assigned by correlation to ^{1}H resonances that were observed in the HSQC spectrum of the fraction. Together, these assignments indicate that the structure of the most abundant oligosaccharide in the plantain XEG fraction is XLGGG, where an underlined G indicates an unbranched β-D-Glc*p* residue that bears an *O*-acetyl substituent at O-6. MALDI-TOFMS analysis (Table 3) was consistent with this interpretation, but also indicated the presence of smaller amounts of oligosaccharides such as XXGGG (*m*/*z* 1202 in the XEG-fraction) that lack β-D-Gal*p* residues. Other low abundance ions in the spectrum of the KOH-fraction indicated the presence of oligosaccharides such as XXGG (*m*/*z* 956) and GGXLGG (*m*/*z* 1442) produced by XEG-catalyzed cleavage of alternative sites exposed by O-deacetylation (see below). ^{1}H NMR integration data (Table 4) of the plantain XEG fraction are consistent with an XXGGG-type branching structure for plantain XyG. The spectra of basil XGOs were very similar and also consistent with an XXGGG-type backbone (data not shown).

The NMR analysis of the KOH-extracted XyGO fraction from plantain (Table 5) is consistent with the identification of XLGGG as the dominant oligosaccharide

Table 4. ^{1}H NMR integrals for XyG oligosaccharide fractions[a,b]

Shift range	Assignment	Oleander		Plantain		Morning glory	
		KOH[a]	XEG[b]	KOH[a]	XEG[b]	KOH[a]	XEG[b]
5.30–5.25	α-Fuc H-1	0.26	0.26	0.00	0.00	0.00	0.00
5.24–5.20	Reducing α-Glc H-1	0.39	0.36	0.38	0.37	0.39	0.30
5.195–5.155	α-Ara H-1 α-Xyl H-1 (L)	1.02	0.83	1.06	0.77	0.87	0.97[c]
5.155–5.120	α-Xyl H-1 (L+F+F)	0.34	0.36	0.00	0.00	0.00	0.00
5.110–5.075	α-Xyl H-1 (S)	0.61	0.16	0.00	0.00	0.86	0.73
5.075–5.040	α-Xyl H-1 (S)	0.00	0.20	0.00	0.00	0.00	0.00
4.970–4.950	α-Xyl H-1 (X—inner)	0.81	0.79	1.03	0.17	1.01	0.22
4.950–5.930	α-Xyl H-1 (X—end)	1.15	1.06	0.10	0.80	0.03	0.99
4.685–4.640	Reducing β-Glc H-1	0.61	0.64	0.62	0.63	0.60	0.69
4.635–4.600	β-Gal H-1 (F)	0.25	0.26	0.00	0.00	0.00	0.00
4.640–4.580	β-Glc H-6 G (acetylated)	0.00	0.00	0.00	1.93	0.00	1.86
4.595–5.480	β-Hex H-1 Fuc H-5	4.17	4.08	5.51	4.96	3.89	4.97
Calculated	Total reducing	1.00	1.00	1.00	1.00	0.99	0.86
Calculated	Total Xyl	3.32	3.04	2.19	1.74	1.91	1.89
Calculated	F side chains	0.26	0.26	0.00	0.00	0.00	0.00
Calculated	L side chains	0.50	0.57	1.06	0.77	0.01	0.20[a]
Calculated	S side chains	0.61	0.36	0.00	0.00	0.86	0.64
Calculated	Backbone β-Glc	4.42	4.25	5.45	5.19	4.87	4.98

[a] KOH indicates the oligosaccharide fraction obtained by XEG treatment of the 4 M KOH extract.
[b] XEG indicates the oligosaccharide fraction obtained by XEG treatment of the cell-wall material.
[c] The morning glory XEG-fraction contained a noncarbohydrate contaminant that increased the signal area diagnostic for α-Ara H-1 and α-Xyl H-1 (L).

subunit of the XyG produced by this species. This fraction is somewhat more complex than the XEG-extracted XyGO fraction, as removal of the *O*-acetyl substituents generates a polymeric substrate with three contiguous XEG-susceptible sites in each subunit. However, the middle site appears to be much more readily hydrolyzed by XEG than the other two, leading to the formation of GXLGG as the major XEG-hydrolysis product. The terminal, unsubstituted β-D-Glc*p* residue (indicated as Glc^{d} in Table 5) in this oligosaccharide could be uniquely identified with the spin system having an anomeric proton resonance at δ 4.518, as terminal β-D-Glc*p* residues give rise to a spin system with a distinctive chemical shift pattern. (http://www.ccrc.uga.edu/web/specdb/specdbframe.html) The same is true for the 4-linked β-D-Glc*p* residue (Glc^{a}, H-1 δ 4.353), the β-D-Glc*p* residue bearing an α-D-Xyl*p* side chain (Glc^{c}, H-1 δ 4.558), the β-D-Glc*p* residue bearing a β-D-Gal*p*-(1→2)-α-D-Xyl*p* side chain (Glc^{b}, H-1 δ 4.551), and the reducing α- and β-D-Glc*p* residues (α-Glc^{r}, H-1 δ 5.221 and β-Glc^{r}, H-1 δ 4.658). Thus, the main component of the KOH-extracted XGO fraction from plantain leaves contains a terminal β-D-Glc*p* residue, an internal 4-linked β-D-Glc*p* residue, two 4,6-linked β-D-Glc*p* residues, and a reducing D-Glc*p* residue. Heterogeneity of the XGO sample prepared from the plantain KOH fraction made it difficult to unambiguously establish the sequence of these residues directly from the NMR data. However, when oligoglycosyl alditols prepared by reduction of the plantain KOH fraction were analyzed by ^{1}H NMR spectroscopy, a characteristic resonance was observed at a chemical shift (δ 4.595), diagnostic for the presence of an unbranched (4-linked) β-D-Glc*p* residue that is directly attached to the alditol. H-1 resonances of branched (4,6-linked) β-D-Glc*p* residues in this position have chemical shifts greater than δ 4.61. When viewed in light of the sequence XLGGG assigned to the major component of the XEG-extracted XGO plantain fraction (see above), these results indicate that the major component of the KOH-extracted XGO fraction is GXLGG.

MALDI-TOFMS analyses of plantain-leaf XGOs (Table 3) were consistent with the assignment of XLGGG as the major component of the XEG-extracted fraction and GXLGG as the major component of the KOH-extracted fraction. Less abundant ions in the MALDI-TOF spectrum of the XEG-extracted fraction had *m*/*z* values indicating the presence of monoacetylated fragments (GXXGG, XLGG, and XXGGG) and a diacetylated fragment that lacked the galactosyl residue (XXGGG). Low-abundance ions in the MALDI-TOF spectrum of the KOH-extracted fraction had *m*/*z* values consistent with the presence of fragments produced by cleavage of β-glucopyranosyl linkages that become XEG-susceptible upon O-deacetylation (GXXG, XXGG, GXXGG, XLGG, GXLG, XXGGG, GGXLGG).

Morning glory (*Ipomoea purpurea*), another lamiid species (order Solanales, family Convolvulaceae) also produces a XyG with an unusual branching structure. ^{1}H NMR signal integration (Table 4) and inspection of the resonances diagonostic for the attachment of

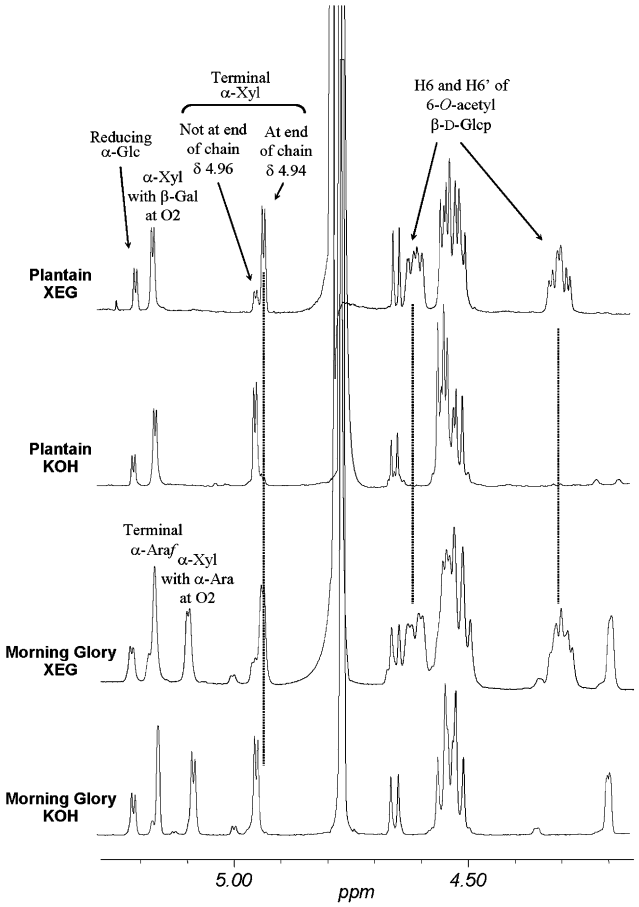

Figure 3. ^{1}H NMR spectra of XyGO fractions from plantain and morning glory. Integration of the H-6 and H-6′ resonances of 6-*O*-acetyl-β-D-Glc*p* residues indicates that each of the oligosaccharides generated by XEG-treatment of plantain and morning glory cell walls contains (on average) two *O*-acetyl substituents.

O-acetyl substituents (Fig. 3, Table 5) indicate that the most abundant XyGO in the morning glory XEG fraction contains two β-D-Glc*p* residues having an *O*-acetyl substituent at O-6, and that the β-D-Glc*p* residue at the nonreducing end of the main chain bears a terminal α-D-Xyl*p* residue at O-6 (α-D-Xyl*p* H-1, δ 4.94). ^{1}H NMR resonances (Table 5) of the most abundant XyGO in the morning glory XEG fraction were assigned by 2D NMR analysis, as described above for the plantain XEG fraction. The resulting glycosyl composition and sequence information allowed the structure of this XGO to be assigned as XSGGG, where again an underlined G represents a 6-*O*-acetyl-β-D-Glc*p* residue. MALDI-TOFMS analysis (Table 3) indicated the presence of XSGGG as the main component, along with small amounts of XXGGG, SSGGG, the monoacetylated oligosaccharide XSGG, and several nonacetylated oligosaccharides (GXSG, XSGGG, GXSGG, and GXSGGG).

The morning glory KOH fraction was more complex than the morning glory XEG fraction, due to the presence of three contiguous XEG-susceptible sites in the polysaccharide after base-catalyzed O-deacetylation. The spin systems corresponding to the major component of the morning glory KOH fraction were assigned (Table 5), as described above for the plantain KOH fraction. This analysis indicated that, as in the plantain KOH fraction, the most abundant XyGO in the morning glory KOH fraction has an unsubstituted β-D-Glc*p* residue at the end of the main chain and an unbranched β-D-Glc*p* residue directly linked to the reducing β-D-Glc*p* residue. In this case, the sequence GXSGG was confirmed by the observation of interglycosidic NOEs (Table 6). Furthermore, the ^{1}H NMR spectrum of the borohydride-reduced morning glory KOH fraction indicated that its major component was GXSGGol, which had previously been isolated as a minor component of the mixture obtained by reduction of the products generated by nonspecific endoglucanase treatment of XyG from tomato cell culture,[9] allowing its ^{1}H NMR resonances to be partially assigned at that time. MALDI-TOFMS analysis (Table 3) was consistent with the presence of GXSGG as the major component, along with smaller amounts of GSSGG and a fragment (GXSG) that arose via cleavage of alternative glycosidic bonds that become XEG-susceptible upon O-deacetylation. Together, the spectroscopic results indicate that morning glory XyG has the same XXGGG-type branching pattern that was identified in plantain XyG. The only significant difference is that morning glory XyG has an α-L-Ara*f*-(1→2)-α-D-Xyl*p*- side chain, where an αβ-D-Gal*p*-(1→2)-α-D-Xyl*p*- side chain is present in the plantain and basil XyGs.

2.3. Conclusions

All of the Campanulid species examined produce typical fucose-containing XXXG-type XyGs, but Lamiid species produce unusual XXGG or XXGGG-type XGs. Plants in the Convovulaceae, Solanaceae, and Oleaceae families produce XyGs that contain arabinosyl residues but no fucosyl residues. *Plantago major* (family Veronicaceae) and *Ocimum basilicum* (family Lamiaceae) both have a repeating XXGGG-type core containing five glucosyl residues, two of which are branched and two of which bear *O*-acetyl substituents. Neither species has fucosyl or arabinosyl residues. *Ipomea purpurea* (family Convovulaceae) has the same XXGGG-type branching and O-acetylation pattern as *Plantago major* and *Ocimum basilicum*, but contains terminal α-Ara*f* residues rather than terminal β-Gal*p* residues. Plant species in the family Solanaceae produce XXGG-type xyloglucans that contain a basic repeating core of four glucose subunits, two of which are branched. One of the unbranched glucose residues is typically acetylated at O-6. Solanaceous xyloglucans also lack fucose but contain arabinose.

Table 5. ^{1}H NMR assignments for XXGGG-type XyGOs from plantain and morning glory[a]

Residue	H-1	H-2	H-3	H-4	H-5	H-5ax	H-6	H-6′
XLGGG (Plantain—XEG extract)								
α-Glc^{r}	5.217	3.575	3.812	3.621	3.945	—	3.863	3.863
β-Glc^{r}	4.655	3.279	3.620	3.625	3.60	—	3.804	3.945
β-Glc^{a}	4.548	3.370	3.662	3.732	3.840	—	4.293	4.620
β-Glc^{b}	4.525	3.385	3.662	3.791	3.845	—	4.311	4.608
β-Glc^{c}	4.512	3.407	3.655	3.655	3.890	—	3.915	3.971
β-Glc^{d}	4.535	3.343	3.515	3.523	3.696	—	3.778	3.940
α-Xyl^{c}	5.180	3.670	3.915	3.65	3.720	3.577	—	—
α-Xyl^{d}	4.941	3.541	3.734	3.621	3.715	3.552	—	—
β-Gal^{c}	4.553	3.613	3.665	3.925	3.687	—	3.78	3.78
Ac^{a}	2.149							
Ac^{b}	2.152							
XSGGG (Morning glory—XEG extract)								
α-Glc^{r}	5.219	3.575	3.814	3.624	3.944	—	3.866	3.866
β-Glc^{r}	4.655	3.282	3.615	3.630	3.595	—	3.806	3.947
β-Glc^{a}	4.548	3.370	3.660	3.730	3.844	—	4.293	4.619
β-Glc^{b}	4.520	3.379	3.652	3.779	3.844	—	4.308	4.609
β-Glc^{c}	4.504	3.392	3.650	3.685	3.839	—	3.948	3.948
β-Glc^{d}	4.535	3.328	3.510	3.520	3.700	—	3.775	3.941
α-Xyl^{c}	5.099	3.573	3.855	3.666	3.729	3.560	—	—
α-Xyl^{d}	4.939	3.544	3.731	3.617	3.714	3.542	—	—
α-Ara^{c}	5.170	4.196	3.936	4.077	3.844	—	3.711	—
Ac^{a}	2.147							
Ac^{b}	2.150							
GXLGG (Plantain—KOH extract)								
α-Glc^{r}	5.221	3.547	3.823	3.639	3.946	—	3.870	3.870
β-Glc^{r}	4.658	3.279	3.63	3.65	3.591	—	3.806	3.952
β-Glc^{a}	4.535	3.380	3.66	3.66	3.628	—	3.826	3.980
β-Glc^{b}	4.551	3.397	3.661	3.739	3.818	—	3.897	4.010
β-Glc^{c}	4.558	3.401	n.a.	n.a.	3.900	—	3.90	3.974
β-Glc^{d}	4.518	3.322	3.507	3.412	3.482	—	3.731	3.915
α-Xyl^{b}	5.175	3.675	3.904	3.66	3.728	3.580	—	—
α-Xyl^{c}	4.959	3.543	3.726	3.625	3.70	3.56	—	—
β-Gal^{c}	4.559	3.615	n.a.	3.921	n.a.	—	n.a.	n.a.
GXSGG (Morning glory—KOH extract)								
α-Glc^{r}	5.221	3.575	3.822	3.641	3.943	—	n.a.	n.a.
β-Glc^{r}	4.658	3.279	3.64	3.64	3.593	—	3.806	3.949
β-Glc^{a}	4.534	3.368	3.66	3.70	3.620	—	3.817	3.979
β-Glc^{b}	4.541	3.398	3.66	3.68	3.839	—	3.948	3.948
β-Glc^{c}	4.557	3.382	3.663	3.736	3.808	—	3.893	4.007
β-Glc^{d}	4.517	3.321	3.506	3.412	3.485	—	3.731	3.916
α-Xyl^{b}	5.091	3.570	3.850	3.666	3.727	3.550	—	—
α-Xyl^{c}	4.957	3.544	3.725	3.625	3.70	3.565	—	—
α-Ara^{c}	5.168	4.196	3.932	4.080	3.843	3.710	—	—

[a] Superscripts a, b, c, d, and r indicate the position of the residue vis-a-vis the reducing end of the oligosaccharide, that is, the backbone structure sequence is Glc^{d}-Glc^{c}-Glc^{b}-Glc^{a}-Glc^{r}. The underlined residues (β-Glc^{a} and β-Glc^{b}) in the XEG-extracts bear an *O*-acetyl substituent at O-6. Resonances that were not assigned are marked 'n.a.'.

The difference in NMR signal intensity for resonances at δ 4.94 and δ 4.96 that are observed when XEG and KOH-extracted samples are compared provides a straightforward diagnostic tool for determining xyloglucan branching patterns. A signal at δ 4.94 in the XEG-extracted sample indicates the presence of a terminal α-D-Xyl*p* residue at O-6 of the nonreducing end β-D-Glc*p* residue of the backbone. The presence of either an α-D-Xyl*p* residue or an acetyl substituent at O-6 of β-D-Glc*p* residues in the backbone inhibit XEG activity at that site. Thus, KOH extraction hydrolyzes *O*-acetyl substituents and exposes backbone sites to cleavage by XEG and other endoglucanases, and a decreased δ 4.940 signal upon treatment with alkali (as in KOH extraction) before XEG-catalyzed generation of oligosaccharide fragments indicates that the xyloglucans have two or more adjacent unbranched β-D-Glc*p* residues in the backbone. In contrast, the presence of an XXXG-type branching structure is indicated if the intensity of the δ 4.940 signal remains relatively unchanged when the XEG- and KOH-extracted materials are compared.

Table 6. Interglycosidic scalar and NOE connectivities for the oligosaccharides[a]

Nucleus (δ)	Nucleus (δ)	Type
XLGGG (Plantain XEG)		
Glc^{c} H-1 (4.513)	Glc^{b} H-4 (3.790)	NOE
Glc^{b} H-1 (4.529)	Glc^{a} H-4 (3.731)	NOE
Glc^{d} H-1 (4.535)	Glc^{c} H-4 (3.656)[e]	NOE
Glc^{a} H-1 (4.548)	Glc^{r} H-4 (3.62)[e,f]	NOE
Gal^{c} H-6 (4.556)	Xyl^{c} H-2 (3.670)	NOE
Xyl^{d} H-1 (4.942)	Glc^{d} H-6 (3.774)	NOE
Xyl^{d} H-1 (4.942)	Glc^{d} H-6′ (3.940)	NOE
Xyl^{c} H-1 (5.180)	Glc^{c} H-6 (3.917)	NOE
Xyl^{c} H-1 (5.180)	Glc^{c} H-6′ (3.970)	NOE
Glc^{c} H-1 (4.513)	Glc^{b} H-4 (3.791)	gCOSY
Glc^{b} H-1 (4.526)	Glc^{a} H-4 (3.734)	gCOSY
XSGGG (Morning glory XEG)		
Glc^{c} H-1 (4.502)	Glc^{b} H-4 (3.782)	gCOSY
Glc^{b} H-1 (4.518)	Glc^{a} H-4 (3.731)	gCOSY
Glc^{d} H-1 (4.538)	Glc^{c} H-4 (3.685)	gCOSY
Glc^{a} H-1 (4.547)	Glc^{r} H-4 (3.624)[f]	gCOSY
GXSGG (Morning glory KOH)		
Glc^{d} H-1 (4.517)	Glc^{c} H-6 (4.004)[g]	NOE
Glc^{d} H-1 (4.517)	Glc^{c} H-6′ (3.890)[g]	NOE
Glc^{d} H-1 (4.517)	Glc^{c} H-4 (3.735)	NOE
Glc^{c} H-1 (4.557)	Glc^{b} H-6 (3.947)[g]	NOE
Glc^{c} H-1 (4.557)	Glc^{b} H-6′ (3.810)[g]	NOE
Glc^{c} H-1 (4.557)	Glc^{b} H-4 (3.68)[e]	NOE
Glc^{b} H-1 (4.541)	Glc^{a} H-4 (3.70)[e]	NOE
Glc^{a} H-1 (4.533)	Glc^{r} H-4 (3.642)	NOE
Xyl^{c} H-1 (4.955)	Glc^{c} H-6 (3.890)	NOE
Xyl^{c} H-1 (4.955)	Glc^{c} H-6′ (4.005)	NOE
Xyl^{b} H-1 (5.091)	Glc^{b} H-6/H-6′ (3.946)	NOE
Ara^{b} H-1 (5.167)	Xyl^{b} H-2 (3.571)	NOE

[a] Superscripts a, b, c, d, indicate the position of the residue vis-à-vis the reducing end (see Table 5); [e]Crosspeak is in a crowded region of the spectrum. [f]Crosspeak is distorted, probably due to overlap of crosspeaks arising from two different anomeric forms of the reducing Glc residue. [g]As previously noted, weak NOEs that correlate H-1 of some β-D-Glc*p* residues to H-6 of the β-D-Glc*p* aglycon can sometimes be observed. Although these NOEs must be interpreted with care (they do not indicate a (1→6)-linkage), they provide sequence information for the β-(1→4)-linkage.

The common fucosylated XXXG-type xyloglucan structure is, for the most part, highly conserved throughout the plant kingdom, suggesting that the presence of fucosyl residues gives the plant a selective advantage. Somewhat surprisingly, ablation of the gene encoding the fucosyl transferase responsible for adding fucosyl residues to XyG in *A. thaliana* does not produce a significant phenotype when plants are grown under nonstressed conditions.[8] Several species of plants produce xyloglucans that lack fucose, but they appear to compensate by varying other structural features. This hypothesis is supported by the observation that all plants examined have at least one of the following features: (1) side chains terminated by fucosyl residues (all Gymnosperms, Rosids, and Campanulid Asterids examined); (2) side chains terminated by arabinosyl residues (Lamiid species in the Convolvulaceae, Solanaceae, and Oleaceae families); (3) an unusual (XXGGG-type) branching pattern in which the basic repeating core consists of a cellopentaose backbone with two side chains (Lamiid species in the Convovulaceae, Lamiaceae and Veronicaceae families). Several of the structural features listed are present in one species, *Nerium oleander*, a Lamiid in the order Gentianales. The combination of diverse structural features in oleander xyloglucan suggests that this species may bridge an evolutionary gap between Lamiid species and plant species with more typical XyG structures. This hypothesis is consistent with recent analyses[17] indicating that divergence of the Gentianales occurred earlier than other Lamiid orders, which produce more diverse XyG structures.

There is no clear correlation between the proposed diversification date[17] and the presence of the XXGGG-type branching pattern, suggesting that this structural modification may have independently arisen in different Lamiid orders. XyGs in which less than 50% of the β-D-Glc*p* residues in the backbone are branched are also produced by various grass species (family Poaceae, see, e.g., Kato et al.[18]), which are monocotyledonous plants that are distantly related to the Asterids, again suggesting that modification of the backbone branching pattern may have occurred independently in different species. Interestingly, XyGs produced by grass species do not contain significant amounts of α-L-Fuc*p* residues, but have been reported to contain small amounts of L-Ara*f* and/or D-Gal*p* residues, again suggesting that modification of the branching pattern may be an adaptation that compensates for the lack of α-L-Fuc*p* residues in the XyG. Further analysis is required to determine whether regular XXGGG-type branching patterns that are observed in the XyGs produced by some Lamiid species are also characteristic of the XyGs produced by various grass species.

3. Experimental

3.1. Selection of plants

Plants were selected to represent a broad range of Lamiid and Campanulid orders within the subclass Asteridae. Lamiid species included plants from the order Solanales (tomato—*Lycopersicon esculentum*, tobacco—*Nicotiana tabacum*, giant sweet peppers—*Capsicum annuum*, morning glory—*Ipomea purpurea*), the order Lamiales (Plantain—*Plantago major*, Basil—*Ocimum basilicum*), and the order Gentianales (oleander—*Nerium oleander*). Campanulid species included plants from the order Asterales (dusty miller—*Tanacetum ptarmiciflorum*, lettuce—*Lactuca sativa*), and the order Apiales (carrot—*Daucus carota*).

3.2. Preparation of plant cell walls

A typical cell wall preparation was obtained as follows: A 30-g sample of leaf tissue was frozen in liquid nitrogen and ground with a mortar and pestle to a fine powder, which was added to a beaker containing 30 mL of 80% EtOH. The suspension was then disrupted with a polytron homogenizer (Brinkman Instruments), and the mixture was centrifuged for 20 min at approximately 2500*g*. The supernatant was decanted and the pellet was washed twice with aqueous 80% (v/v) EtOH and then with abs EtOH, and collected by centrifugation. (In some preparations, the insoluble residue obtained after EtOH washing was collected by vacuum filtration.) The pellet was then stirred in 30 mL of 1:1 $CHCl_3$–MeOH overnight, collected by filtration through a glass fiber filter (GF/A Whatman), washed with 1:1 $CHCl_3$–MeOH and then with acetone. (For some preparations, the overnight $CHCl_3$–MeOH wash was replaced with a 2-h wash in 100 mL of $CHCl_3$–MeOH.) The resulting AIR, which consists primarily of cell-wall material, was vacuum dried overnight (typical yield, 3–4 g).

3.3. XEG-treatment of AIR

AIR (0.5 g) from each plant species was suspended in 40 mL of 50 mM NaOAc buffer, pH 5, containing 0.01% (w/v) thimerosal and endopolygalacturonase (EPG, 5–10 units, prepared from *Aspergillus niger* and generously provided by Carl Bergmann CCRC) and pectin methyl esterase (PME, 10 units from *Aspergillus oryzae*, Novozymes A/S, Bagsvaerd Denmark) and shaken at 24 °C for 24 h. Solubilized material was collected by vacuum filtration, and the solid residue was extracted a second time with EPG/PME. The solid residue was suspended in 50 mM NaOAc buffer (pH 5) containing 0.01% (w/v) thimerosal, and xyloglucan-specific endoglucanase (XEG, 7.8 units, Novozymes A/S, purified as described by Pauly et al.[19]) was added. The suspension was incubated for 24 h and then filtered through a glass fiber filter (GF/A Whatman). The filtrate, which contained xyloglucan oligosaccharides solubilized by the XEG, was applied to a Supelco LC-18/ODS cartridge (preconditioned by washing with 6 mL of MeOH followed by 15 mL of H_2O). The loaded cartridge was washed with H_2O (20 mL) to remove salts, and xyloglucan oligosaccharides were then eluted with 25% MeOH. MeOH was removed from the eluants by evaporation under vacuum, and the concentrated samples were lyophilized. Xyloglucan oligosaccharides were isolated by size-exclusion chromatography on Superdex 75 (Amersham Biosciences, Uppsala) eluted with aq HCO_2NH_4 (50 mM, pH 5). The refractive index of the eluant was monitored, and oligosaccharide-containing fractions were pooled and lyophilized.

3.4. KOH extraction

The solid residue obtained after XEG treatment of the AIR was suspended in 1 M KOH for 24 h and then recovered by vacuum filtration. The 1 M KOH residue was suspended in 4 M KOH for 24 h and the solubilized material was recovered by filtration, neutralized with glacial HOAc, and dialyzed using 3500 MWCO tubing (Spectrum Laboratories, Rancho Dominguez CA) against 4–6 changes of water (4 L) over 2–3 days. The retentate, which contained polymeric xyloglucan, was lyophilized, and then suspended in 50 mM NaOAc buffer, pH 5. XEG (7.8 units) was added, and the solution was shaken for 24 h (37 °C). The resulting xyloglucan oligosaccharides were isolated by size-exclusion chromatography, as described above.

3.5. Preparation and purification of oleander, plantain, and morning glory XyG oligosaccharides

AIR (2 g) was prepared from leaves and treated as described above with EPG and PME to solubilize pectins. The solid residue was treated with XEG as described above, and after a 24 h incubation, the suspension was filtered through glass fiber (Whatman GF/A). Then, 3 vol of 95% EtOH were added to the filtrate, and the resulting precipitate was removed by centrifugation (10 min at 3000*g*). The supernatant containing XyG oligosaccharides was concentrated by rotary evaporation to remove the EtOH. XyG oligosaccharides were further purified by SEC on a Sephadex G-25 column (2.5×90 cm) eluted with deionized H_2O. Conductance was measured and anthrone assays were performed for each 4-mL fraction collected. Salt-free fractions containing carbohydrate were pooled and lyophilized. Ion-exchange chromatography was used to remove contaminating pectic material as follows: the lyophilized material was dissolved in 10 mL of H_2O, 30 mL of 10 mM imidazole HCl buffer (pH 7) was added, and the sample was loaded onto a 50 mL Q-Sepharose column equilibrated with the imidazole buffer. The column was eluted with 100 mL of the same buffer, and 10-mL fractions were collected. Carbohydrate-containing fractions (as determined by the anthrone assay) were pooled and lyophilized.

The solid residue obtained after XEG treatment was extracted with 1 M, followed by 4 M, KOH as described above. The 4 M KOH-soluble extract was dialyzed, lyophilized, dissolved in 20 mM NaOAc buffer (pH 5) and treated with XEG, as described above. The resulting xyloglucan oligosaccharides obtained were reduced to the corresponding oligoglycosyl alditols by dissolving the sample in 10 mL of 1 M ammonia containing 10 mg/mL $NaBH_4$. The reaction was stopped after 1 h at room temperature by addition of HOAc to a final pH of 3.0. The resulting oligoglycosyl alditols were desalted on Sephadex G-25, as described above. The

purified oligosaccharides were analyzed before and after reduction to the corresponding alditols by MALDI-TOF mass spectrometry and 1D and 2D NMR spectroscopy.

3.6. HPLC of oligosaccharides

XyG oligosaccharides in the oleander XEG fraction and XyG oligoglycosyl alditols prepared by reduction of oligosaccharides in the oleander KOH fraction were further purified by reversed-phase HPLC. Samples were dissolved in 1 mL of H_2O, and the components were separated on an octadecylsilyl (C_{18}) column (Hibar Lichrosorb RP-18, 25 × 1.0 cm). XGOs were eluted with 15% MeOH (3 mL min^{-1}) and detected by evaporative light scattering (Sedex 55 ELSD, SEDERE, France). For each HPLC run, 200 μL of sample was loaded. Fractions were manually collected and concentrated by rotary evaporation to remove MeOH and analyzed by MALDI-TOF mass spectrometry and NMR spectroscopy.

3.7. Matrix-assisted laser-desorption/ionization time-of-flight mass spectrometry (MALDI-TOFMS)

MALDI-TOF mass spectra were recorded using a Hewlett–Packard LDI 1700 XP spectrometer operated at an accelerating voltage of 30 kV, an extractor voltage of 9 kV, and a source pressure of approx 8×10^{-7} Torr. The matrix was prepared by mixing (1:1 v/v) 2,5-dihydroxybenzoic acid (DHB, 0.2 M) and 1-hyroxyisoquinoline (HIC, 0.06 M), both in 50% aq MeCN.

3.8. Nuclear magnetic resonance (NMR) spectroscopy

Purified samples were dissolved in D_2O (0.6 mL, 99%; Cambridge Isotope Laboratories, Andover MA) and transferred to a 5-mm NMR tube. NMR spectra were recorded at 298 K using a Varian Inova-600 MHz NMR spectrometer. Chemical shifts were measured relative to internal acetone at δ 2.225. Two-dimensional gCOSY, NOESY, TOCSY, gHSQC, and HMBC spectra[20] were recorded using standard pulse sequences provided by Varian. In order to observe very weak scalar coupling interactions, high-resolution gCOSY experiments[16] were obtained with 4k data points in the directly detected dimension and 800–1024 time increments in the indirectly detected dimension, and data was apodized in both dimensions using a sine-squared function. Data were processed using MestRe-C (University of Santiago, Spain).

Acknowledgments

This research was funded by the U.S. Department of Energy (grant no. DE-FG05-93ER20220) and by the U.S. Department of Energy-funded Center for Plant and Complex Carbohydrates (grant no. DE-FG05-93ER20097). The authors would like to thank Novozymes A/S for the xyloglucan-specific endoglucanase (XEG) and Dr. Carl Bergmann of the CCRC for pectin-degrading enzymes used in this study.

References

1. O'Neill, M. A.; York, W. S. The composition and structures of primary cell walls. In *The Plant Cell Wall*; Rose, J. K. C., Ed.; CRC Press: Boca Raton, FL, 2003; Vol. 8, pp 1–54.
2. Cosgrove, D. J. *Plant Physiol. Biochem.* **2000**, *38*, 109–124.
3. Levy, S.; Staehelin, L. A. *Curr. Opin. Cell Biol.* **1992**, *4*, 856–862.
4. Whitney, S. E. C.; Gothard, M. G. E.; Mitchell, J. T.; Gidley, M. J. *Plant Physiol.* **1999**, *121*, 657–664.
5. Vincken, J.-P.; York, W. S.; Beldman, G.; Voragen, A. G. *Plant Physiol.* **1997**, *114*, 9–13.
6. Buckeridge, M. S.; Crombie, H. J.; Mendes, C. J. M.; Reid, J. S. G.; Gidley, M. J.; Vieira, C. C. J. *Carbohydr. Res.* **1997**, *303*, 233–237.
7. Fry, S. C.; York, W. S.; Albersheim, P.; Darvill, A. G.; Hayashi, T.; Joseleau, J.-P.; Kato, Y.; Lorences, E. P.; Maclachlan, G. A.; McNeil, M.; Mort, A. J.; Reid, J. S. G.; Seitz, H. U.; Selvendran, R. R.; Voragen, A. G. J.; White, A. R. *Physiol. Plant.* **1993**, *89*, 1–3.
8. Perrin, R. M.; Jia, Z. H.; Wagner, T. A.; O'Neill, M. A.; Sarria, R.; York, W. S.; Raikhel, N. V.; Keegstra, K. *Plant Physiol.* **2003**, *132*, 768–778.
9. York, W. S.; Kolli, V. S. K.; Orlando, R.; Albersheim, P.; Darvill, A. G. *Carbohydr. Res.* **1996**, *285*, 99–128.
10. Jia, Z.; Cash, M.; Darvill, A. G.; York, W. S. *Carbohydr. Res.* **2005**, *340*, in this issue, please see doi:10.1016/j.carres.2005.04.015.
11. Pauly, M.; Albersheim, P.; Darvill, A. G.; York, W. S. *Plant J.* **1999**, *20*, 629–639.
12. York, W. S.; van Halbeek, H.; Darvill, A. G.; Albersheim, P. *Carbohydr. Res.* **1990**, *200*, 9–31.
13. Jia, Z. H.; Qin, Q.; Darvill, A. G.; York, W. S. *Carbohydr. Res.* **2003**, *338*, 1197–1208.
14. Sims, I. M.; Munro, S. L.; Currie, G.; Craik, D.; Bacic, A. *Carbohydr. Res.* **1996**, *293*, 147–172.
15. Vierhuis, E.; York, W. S.; Kolli, V. S. K.; Vincken, J.-P.; Schols, H. A.; Van Alebeek, G. J. W. M.; Voragen, A. G. J. *Carbohydr. Res.* **2001**, *332*, 285–297.
16. Otter, A.; Bundle, D. R. *J. Magn. Reson. Ser. B* **1995**, *109*, 194–201.
17. Bremer, K.; Fris, E. M.; Bremer, B. *Systemat. Biol.* **2004**, *53*, 496–505.
18. Kato, Y.; Ito, S.; Iki, K.; Matsuda, K. *Plant Cell Physiol.* **1982**, *23*, 351–364.
19. Pauly, M.; Andersen, L. N.; Kauppinen, S.; Kofod, V.; York, W. S.; Albersheim, P.; Darvill, A. G. *Glycobiology* **1999**, *9*, 93–100.
20. Kessler, H.; Gehrke, M.; Griesinger, C. *Angew. Chem., Int. Ed. Engl.* **1988**, *27*, 490–536.
21. Kakegawa, K.; Edashige, Y.; Ishii, T. *Phytochemistry* **1998**, *47*, 767–771.
22. Kato, Y.; Katsuhiro, I.; Matsuda, K. *Agric. Biol. Chem.* **1981**, *45*, 2745–2753.

23. Kato, Y.; Matsuda, K. *Plant Cell Physiol.* **1985**, *26*, 437–445.
24. Watanabe, T.; Shida, M.; Murayama, T.; Furuyama, Y.; Nakajima, T.; Matsuda, K. *Carbohydr. Res.* **1984**, *129*, 229–242.
25. Kato, Y.; Nevins, D. J. *Plant Cell Physiol.* **1991**, *32*, 713–720.
26. Ohsumi, C.; Hayashi, T. *Plant Cell Physiol.* **1994**, *35*, 963–967.
27. Braccini, I.; Herve du Penhoat, C.; Michon, V.; Goldberg, R.; Clochard, M.; Jarvis, M. C.; Huang, Z. H.; Gage, D. A. *Carbohydr. Res.* **1995**, *276*, 167–181.
28. Hayashi, T.; Delmer, D. P. *Carbohydr. Res.* **1988**, *181*, 273–277.
29. Hayashi, T.; Takeda, T. *Biosci. Biotechnol. Biochem.* **1994**, *58*, 1707–1708.
30. Renard, C. M. G. C.; Lomax, J. A.; Boon, J. J. *Carbohydr. Res.* **1992**, *232*, 303–320.
31. Watt, D. K.; Brasch, D. J.; Larsen, D. S.; Melton, L. D. *Carbohydr. Polym.* **1999**, *39*, 165–180.
32. Hantus, S.; Pauly, M.; Darvill, A. G.; Albersheim, P.; York, W. S. *Carbohydr. Res.* **1997**, *304*, 11–20.
33. Buckeridge, M. S.; Rocha, D. C.; Reid, J. S. G.; Dietrich, S. M. C. *Physiol. Plant.* **1992**, *86*, 145–151.
34. Hayashi, T.; Kato, Y.; Matsuda, K. *Plant Cell Physiol.* **1980**, *21*, 1405–1418.
35. Huisman, M. M. H.; Weel, K. G. C.; Schols, H. A.; Voragen, A. G. J. *Carbohydr. Polym.* **2000**, *42*, 185–191.
36. Kooiman, P. *Rec. Trav. Chim.* **1961**, *80*, 849–865.
37. Kato, Y.; Matsuda, K. *Agric. Biol. Chem.* **1980**, *44*, 1759–1766.
38. Matsushita, J.; Kato, Y.; Matsuda, K. *Agric. Biol. Chem.* **1985**, *49*, 1533–1534.
39. Kato, Y.; Watanabe, T. *Biosci. Biotechnol. Biochem.* **1993**, *57*, 1591–1592.
40. Ray, B.; Loutelier-Bourhis, C.; Lange, C.; Condamine, E.; Driouich, A.; Lerouge, P. *Carbohydr. Res.* **2004**, *339*, 201–208.
41. Pauly, M.; Eberhard, S.; Albersheim, P.; Darvill, A.; York, W. S. *Planta* **2001**, *214*, 67–74.
42. Ring, S. G.; Selvendran, R. R. *Phytochemistry* **1981**, *20*, 2511–2519.
43. Kiefer, L. L.; York, W. S.; Darvill, A. G.; Albersheim, P. *Phytochemistry* **1989**, *28*, 2105–2107.